International Journal of Automotive Technology, Vol. 6, No. 3, pp. 229–234 (2005)

1229–9138/2005/021–05

STUDY ON DYNAMIC BEHAVIOUR IN 3PB DUCTILE STEEL SPECIMEN APPLIED BY THE IMPACT LOAD

M. S. HAN[1)*], J. U. CHO[2)] and A. BERGMARK[3)]

[1)]Faculty of Mechanical and Automotive Engineering, Keimyung University, Daegu 704-701, Korea
[2)]Faculty of Mechanical and Automotive Engineering, Kongju National University, Cheonan 330-717, Korea
[3)]Department of Solid Mechanics, Lund Institute of Technology, Box 118, S-221 00, Lund, Sweden

(Received 12 May 2004; Revised 18 September 2004)

ABSTRACT–The dynamic crack growth in ductile steel is investigated by means of the impact loaded 3 point bending (3PB) specimens. Results from experiments and numerical simulations are compared to each other. A modified 3PB specimen designed with the reduced width at its ends has been developed in order to avoid the initial compressive loading of the crack tip and also to avoid the uncertain boundary conditions at the impact heads. Numerical simulations of the experiments are made by using a finite element method (FEM) code, ABAQUS. The high speed photography is used to obtain the crack growth and the data of the crack tip opening displacement (CTOD). The direct measurements of the relative rotations of two specimen halves are made by using the Moire interference pattern.

KEY WORDS : Dynamic fracture, Moire interference pattern, Crack tip opening displacement, Visco-plastic properties

1. INTRODUCTION

Earlier investigations have been made on the dynamic behavior of the impact loaded 3PB specimen and the influence of the boundary conditions at impact points (Kanninen, 1979; Van, 1984; Wihlborg, 1985; Nakamura *et al.*, 1986; Bergmark and Kao, 1991). Nowdays, the dynamic analysis is also applied by the area of automobile (Jang and Chae, 2000; Song *et al.*, 2002; Cheon and Meguid, 2004). It was found that the specimen behavior is very much influenced by the boundary conditions between the hammer and the specimen at impact points (Bergmark and Kao, 1991).

As the numbers of automobiles are increased and are popular to the people recently, the safety which can prevent against the accidents becomes concerned very much. The study of design by the particular consideration about the accidents occurred at the impact is nowadays progressed very actively. As the load occurred at impact delivers for a short time, the structure becomes deformed and destructed.

Therefore, the precise analysis about the impact problem is very important at the standpoint of the structural safety and the impact force which is concentrated instantaneously is directly due to the deformation of the car body at the moment of the collision of car. As the circumstances of impacts are various in fact and the intensities become different according to the characteristics of material, the configurations of plastic regions become different. Among various materials, the ductile specimen deforms plastically at the impact point, especially at higher impact velocities. The circular shaped impact heads form the circular indents, which in turn work as guides for the successive deformation of the specimen. The mechanical locking at these indents and the friction between the impact heads and the specimen were shown to have the pronounced influence on the response of the specimen. Furthermore, the transition from ductile fracture surfaces to partly brittle fracture surfaces of the specimen 18 mm thick at the impact velocity 15 m/s was also found for the impact velocities 30 m/s and 45 m/s. Brittle fracture surfaces were found in the center part and ductile shear lips at the outer parts of the fracture surfaces at the two higher impact velocities. The present investigation is focused on finding the way either to eliminate the uncertainty in defining the boundary conditions or to eliminate the influence of the uncertain boundary condition. It was decided to reduce the thickness of specimen in order to avoid the transition from ductile to brittle fracture surfaces. The objective here is to study the behavior of purely ductile specimen and the results of this study can be applied to the parameters of the basic design on the nonlinear plastic region at the impact analysis of automobile.

**Corresponding author.* e-mail: sheffhan@kmu.ac.kr

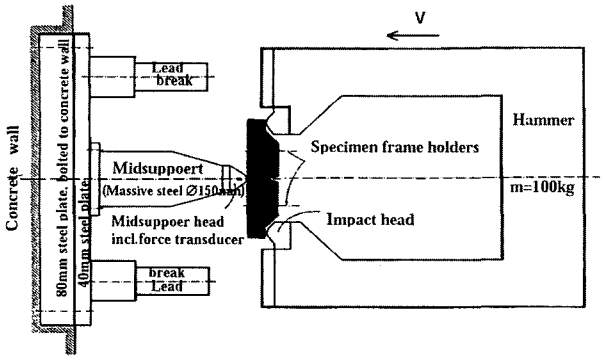

Figure 1. The experimental display.

2. EXPERIMENTS

The experimental display is shown in Figure 1 (Kanninen, 1979). The U-shaped hammer is accelerated to a prescribed velocity and hits the 3PB specimen at its ends. Two hardened and tempered impact heads with cylindrical contact surfaces are attached to the hammer. The experiments presented here were carried out at a temperature of 18°C and with impact velocities of 30.2 m/s and 45.2 m/s. A static test was also carried out with the midpoint loading at the velocity of 50 mm/min.

The dimensions of the new designed specimen are shown in Figure 2. This figure also indicates the longitudinal grid which is milled in the specimen surface for the direct measurement of the relative rotation of two specimen halves by using the Moire interference patterns. The chemical composition of the specimen material is shown in Table 1. The stress-strain relationship from a

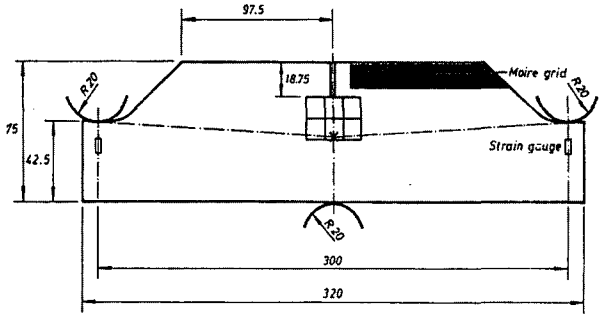

Figure 2. Dimensions of the new designed 3PB specimen [mm].

Table 1. Chemical composition (Wt. Components in %).

C	Si	Mn	P	S	Al	Nb
0.14	0.30	1.41	0.014	0.011	0.045	0.030
V	N	Mo	Cu	Cr	Ni	
0.008	0.005	0.004	0.009	0.02	0.04	

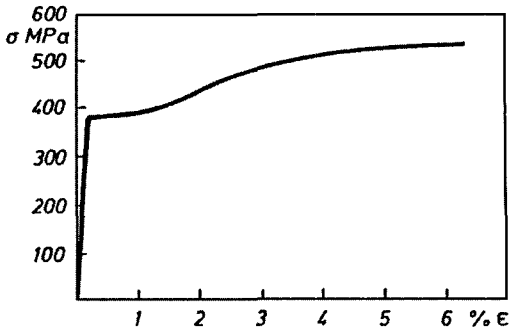

Figure 3. Static tensile test diagram (engineering strain and stress) for SIS2134.

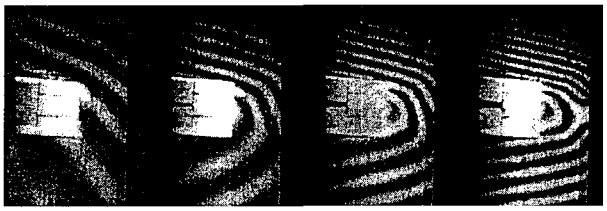

Figure 4. Moire interference pattern.

static tensile test is shown in Figure 3.

The high speed photography is used for the overall recording of the event and for the detailed measurements of the crack initiation and the crack tip opening displacements. A force transducer is incorporated in the mid-support, see Figure 1. The time for impact is detected by the strain gauge attached at the ends of specimen where the hammer hits the specimen. The camera was operated with 160,000 frames per second by the exposure time of 1.0 μs. The relative rotation is calculated from the distance between the Moire interference pattern lines obtained from the high speed photographs. The Moire interference pattern is obtained between the grid milled on the specimen surface and the reference grid which is kept at a distance of 3 mm above the specimen. The reference grid is copied on the transparently self-adhesive plastic sheet which is mounted on the PMMA plate 2 mm thick. The typical recording of the Moire interference pattern is seen in Figure 4.

3. RESULTS FROM THE NUMERICAL SIMULATION

The numerical simulations are made by using the commercial finite element code, ABAQUS (Karlsson and Sorensen, 1989). The material is modeled as the elasto-plastic material using an isotropic hardening von Mises model.

The used mesh is shown in Figure 5. Due to the symmetry, only half of the specimen is modeled. The

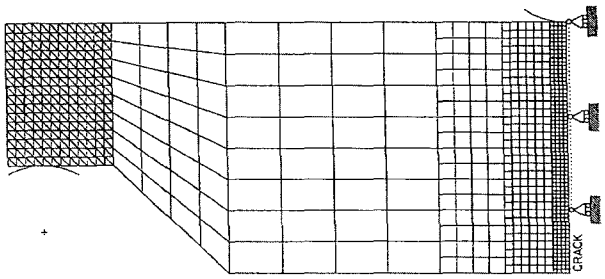

Figure 5. FEM-model for the 3PB specimen with a quarter edge crack.

bilinear plane stress elements of two dimensional four nodes are chosen in the center part of the specimen. The element size is reduced along the crack plane. No concentration of the mesh at the original crack tip was included in order to be able to include the crack propagation in the model. The plastic shear of the end of reduced width specimen may occur. Therefore, a finer mesh is introduced in this area. The plane stress elements of triangular constant strains are used and the mesh alignment is used in order to catch the possible slip lines acting over the corner. Several calculations with the succesively finer mesh at the ends were made. No significant difference between the results using the present model and the model with more coarse mesh was obtained. The impact head and the mid support are modeled as rigid surfaces which work as indenters on the specimen. In order to model the possible loss of contact at the load point and at the mid support, interface elements which allow the separation are introduced along the specimen where the contact is expected. No friction between the impact head and the specimen is included in the model. The mass of node of the impact head is 50 kg which corresponds to the half of the hammer weight. The impact heads are fixed by connecting to the hammer and consequently no motion of the impact head parallel to the front surface of specimen is allowed. Simulations are made with and without crack growth. The crack propagation was modeled according to its history found from the experiments. These simulations were made by using the new boundary option in ABAQUS to release nodes as the function of time along the crack plane. The relative rotation of the specimen halves was determined from the rotation of the front side of specimen. The excessive plastic deformation of the specimen is obtained at the ends of specimen, where the indenters of impact head are about 3 mm deep. The plastic shears of the entire transverse section are obtained at the ends of specimen and the plastic hinges are developed at the midsection of the specimen.

Figure 6 shows the plastic areas after 160 μs. Isostrain curves are shown for equivalent plastic strains from

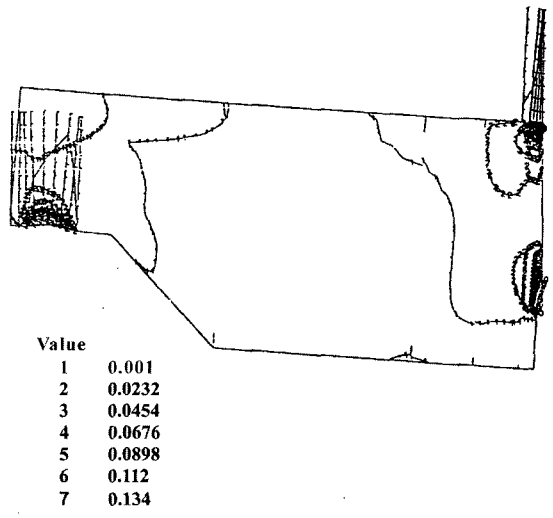

Figure 6. Numerical calculation of the plastic strains at the impact velocity 30.2 m/s after the elapsed time of 160 μs.

0.1%. The key numbers for the curves are as follows; 1:0.1%, 2:2.32%, 3:454%, 4:6.76%, 5:8.98%, 6:11.2%, 7:13.4%, 8:15.6%. The staple diagrams at the impact head and the midsupport indicate the maximum equivalent plastic strain of about 16% at the impact head and about 12% at the midsupport. Simulations are made with the rate dependent material properties according to the Malvern viscoplastic model. The one dimensional form of this model is as follows (Malvern, 1951):

$$\dot{\varepsilon}^{vp}=\beta\left(\frac{\sigma}{\sigma_y}-1\right)^n \tag{1}$$

with the notations

$\dot{\varepsilon}^{vp}$: plastic strain

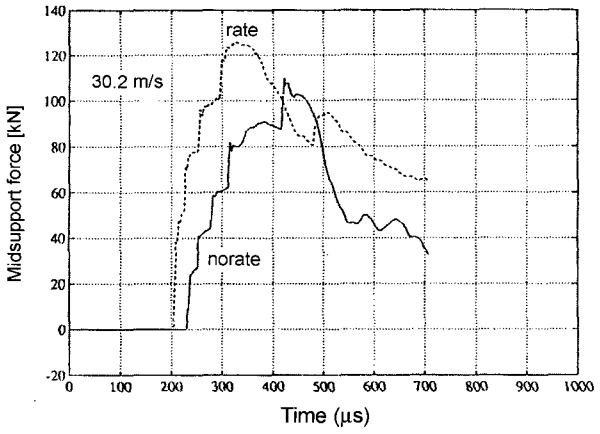

Figure 7. Influence of the viscoplastic material properties on the midsupport force for the impact velocity of 30.2 m/s.

σ : stress
σ_y : yield stress
β, n : viscoplastic parameters

Figure 7 shows the simulation of the midsupport force as the function of time for the case of 30.2 m/s impact velocity. The viscoplastic parameters are chosen as β=4000 and n=2 which are considered to give a moderate viscoplastic influence (Brickstad, 1983). The notations of rate and norate indicate the result from simulations with and without rate depending material properties. The bouncing time is the interval of no contact force at the midsupport between the specimen and the hammer. As is seen in the figure, the introduction of viscoplastic properties decreases the bouncing time of specimen and increases the force growth rate when the contact is established between the midsupport and the specimen.

4. COMPARISON OF EXPERIMENTS AND NUMERICAL SIMULATIONS

In the analysis of ABAQUS, the crack growth is not checked. Because the displacement at the crack tip is released on Y-direction, the crack can be seen to be grown.

Therefore, each node of crack tip is changed whenever the time is elapsed during the crack growth.

In this paper, the crack growth is taken by the photos of the high speed camera per a time interval during the impact experimentally. That time is the period from the moment of the impact until 800 μs. The half length of crack measured by microscope is inputted by this analysis. Each crack is released during the crack growth by using the experimental data. The half length of crack is X coordinate of each crack tip. The nodes from the origin into the coordinate of the node just before the node of crack tip are released by Y-direction when the crack propagates. The mid-support force, the relative rotation, and the crack tip opening displacement are obtained at each time. These data are also drawn by Figures 8 to 13. These crack growths are illustrated in parentheses at these figures.

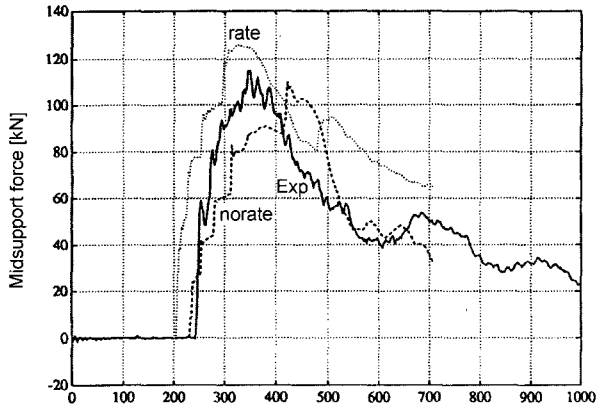

Figure 8. Mid-support force at 30.2 m/s impact velocity for the four different simulations and the experiment. (experiment: full line, simulations, no rate: broken line, rate: dotted line).

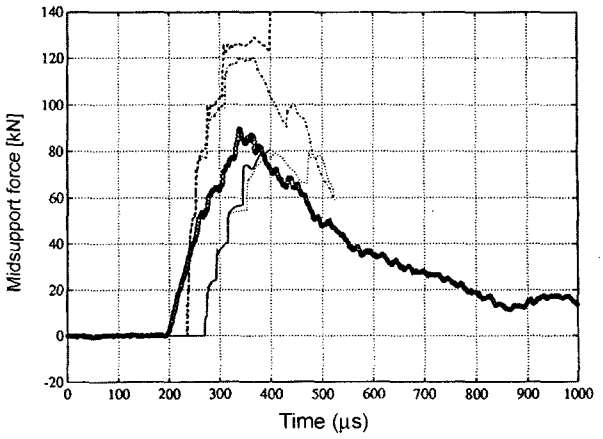

Figure 9. Mid-support force at 45.2 m/s impact velocity for the four different simulations and the experiment. (experiment: thick line, simulations, no rate and no crack growth: full line, no rate and crack growth: dotted line, rate and no crack growth: broken line, rate and crack growth: point line).

The mid-support forces for the four simulations together with the experimental results are shown with impact velocities of 30.2 m/s and 45.2 m/s, respectively in Figure 8 and Figure 9. The simulations including viscoplatic properties are more close to the experimental results. As seen from Figure 8 and Figure 9, the bouncing time in Figure 9 with the impact velocity of 45.2 m/s is shorter than that in Figure 8 with 30.2 m/s experiment. This indicates that the specimen is stiffer at 45.2 m/s experiment by comparing with the 30.2 m/s impact velocity experiment. This fact also means that the viscoplastic property is shown more remarkably at the increasing speed. The simulations are the combinations of with and without rate influence (Brickstad,1983) and with and without crack growth. They are denoted as rate -no rate and crack growth - no crack growth.

The relative rotations as a function of time are shown with the impact velocity of 30.2 m/s in Figure 10. All simulations overestimate the real values with the exception of the small time interval at about 100 μs for the case of no rate. This might be explained by either the underestimation of the plastic deformation at the end of specimen or by the oscillation of supporting wall. The relative rotation as the function of time is shown with impact velocity of 45.2 m/s in Figure 11. The maximum difference between the simulations and the experiment is

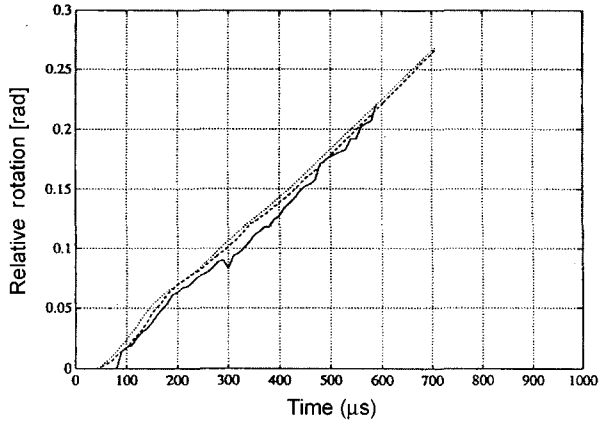

Figure 10. Relative rotation at 30.2 m/s impact velocity for the four different simulations and the experiment. The full drawn line denotes the experiment. (experiment: full line, simulations, no rate: broken line, rate: dotted line).

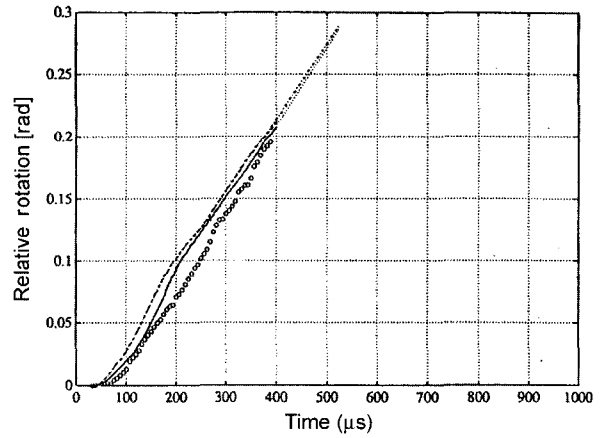

Figure 11. Relative rotation at 45.2 m/s impact velocity for the experiment and the simulations. The experiment is denoted by circles. (experiment: circles, simulations, no rate and no crack growth: full line, no rate and crack growth: dotted line, rate and no crack growth: broken line, rate and crack growth: point line).

obtained at 200 μs. The difference corresponds to the displacement of the midpoint of specimen. The simulations overestimate the bending of the specimen corresponding to the displacement of the midpoint.

The CTODs as the function of time are also shown with impact velocity of 30.2 m/s in Figure 12. CTOD is obtained by the displacement of Y-direction at the crack tip. No difference is found between the simulations with and without crack propagation. As is seen from the figure, the experimental CTODs are close to those of the simulation including the rate influence. Figure 13 shows the CTOD as the function of time with the impact velocity of 45.2 m/s. The best fit by the simulation to the

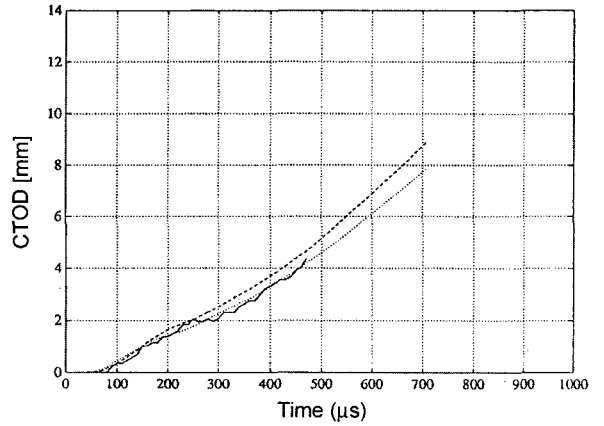

Figure 12. CTOD at 30.2 m/s impact velocity for the four different simulations and the experiment. (experiment: full lin, simulations, no rate: broken line, rate: dotted line).

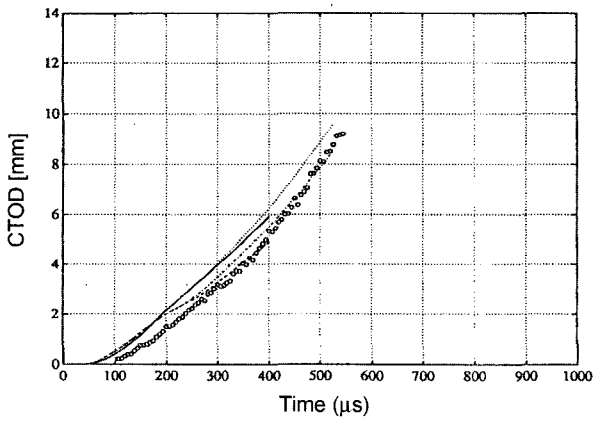

Figure 13. CTOD at 45.2 m/s impact velocity for the four different simulations and the experiment. (experiment: circles, simulations, no rate and no crack growth: full line, no rate and crack growth: dotted line, rate and no crack growth: broken line, rate and crack growth: point line).

experiment is obtained when the viscoplastic and crack propagation properties are included.

5. CONCLUSIONS

The conclusions can be summarized as follows:

(1) The good agreement between the experiments and the numerical simulations was obtained for the case of 30.2 m/s impact loading. The results indicate that the viscoplastic properties are present in the material.

(2) The plastic deformations of the entire transverse area are obtained at three transverse sections. The specimen deformation is very sensitive to the plastic

hardening and viscoplastic properties of the material.

(3) It was found from the 45.2 m/s experiment that the bouncing time is shorter than that in the 30.2 m/s experiment. This indicates that the specimen is stiffer at 45.2 m/s experiment by comparing with the experiment of 30.2 m/s impact velocity. The reduction of bouncing time indicates that the material has the viscoplastic properties and the stiffness is underestimated.

(4) By utilizing these results of analyses, the dangerous condition in which part is subject to take much load and deform can be estimated at the moment of the dynamic fracture of material by impact. And these results are thought to be the important data which can be applied as the assessment of safety on the design of automobile about the impact problem.

REFERENCES

Bergmark, A. and Kao, H. R. (1991). Dynamic crack initiation in 3PB ductile steel specimens. *Technical Report, LUTFD2 TFHF-3041, Lund Institute of Technology,* Sweden, 1–23.

Brickstad, B. (1983). A viscoplastic analysis of rapid crack propagation experiments in steel. *J. Mech. Phys. Soilds* **31, 4,** 307–332.

Cheon, S. S. and Meguid, S. A. (2004). Crush behavior of metallic foams for passenger car design. *Int. J. Automotive Technology* **5, 1,** 47–53.

Jang, I. S. and Chae, D. B. (2000). The derivation of simplified vehicle body stiffness equation using collision analysis. *Trans. Korean Society Automotive Engineers* **8, 4,** 177–185.

Kanninen, M. F. etc. (1979). Dynamic crack propagation under impact loading. *Nonlinear and Dynamic Fracture Mechanics, ASME AMD* **35,** 185–200.

Hibbitt, Karlsson and Sorensen Inc. (1989). ABAQUS Manual. Version 4.8.

Malvern, L. E. (1951). The propagation of longitudinal waves of plastic deformation in a bar of material exhibiting a strain- rate effect. *J. Appl. Mech.* **18,** 203–208.

Nakamura, T., Shih, C. F. and Freund, L. B. (1986). Analysis of a dynamically loaded three- point-bend ductile fracture specimen. *Eng. Frac. Mech.* **25,** 323–339.

Song, J. H., Park, J. M., Chae, H. C., Kang, Y. H. and Yang, S. M. (2002). The estimation of dynamic strength characteristics of high tensile steel by dynamic lethargy coefficient. *Trans. Korean Society Automotive Engineers* **10, 2,** 96–100.

Van Elst, H. G. (1984). Assessment of dynamic fracture propagation resistance at instrumented high velocity gasgun impact tests on SENB-Specimens. *6th International Conference on Fracture* **5,** 3089–3097.

Wihlborg, G. (1985). Design and application of a rig for high energy impact tests. *IUTAM Symposium on MMMHVDF,* 37–47.